Polymer Chemistry

Accepted Manuscript

ROYAL SOCIETY OF CHEMISTRY

www.rsc.org/polymers

High Charge Mobility Polymers Based on a New Di(thiophen-2-yl)thieno[3,2-b]thiophene for Transistors and Solar Cells

Lie Chen[a,b], Feiyan Wu[a], Zhiqiang Deng[a], Linlin Feng[c], Pengcheng Gu[c], Huanli Dong[c], Wenping Hu*[c], Yiwang Chen*[a,b]

[a]College of Chemistry/Institute of Polymers, Nanchang University, 999 Xuefu Avenue, Nanchang 330031, China

[b]Jiangxi Provincial Key Laboratory of New Energy Chemistry, Nanchang University, 999 Xuefu Avenue, Nanchang 330031, China

[c]Institute of Chemistry, Chinese Academy of Sciences, 2 Zhongguancun North First Street, Beijing 100190, China

Corresponding author. Tel.: +86 791 83968703; fax: +86 791 83969561. E-mail: ywchen@ncu.edu.cn (Y. Chen); huwp@iccas.ac.cn (W. Hu)

Lie Chen and Feiyan Wu contributed equally to this work.

Abstract

A novel Donor-Acceptor (D-A) donor di(thiophen-2-yl)thieno[3,2-b]thiophene (DTTT) was designed and synthesized according to the structure of diketopyrrolopyrrole (DPP) acceptor. The random polymers with different ratio of DTTT/DPP, PDTTT-T-DPP_3/7 and PDTTT-T-DPP_4/6, and the alternating polymer PDTTT-DPP were synthesized through the random copolymerization and direct arylation scheme respectively. Although the planarity of DTTT structure is not as good as the DPP molecule, incorporation of DTTT and DPP molecules stimulate the polymers to achieve high hole mobility, as determined by polymer thin film transistors (PTFTs) devices, as well as yield fine power conversion efficiencies in polymer solar cell. Especially for the PDTTT-T-DPP_3/7, the PTFTs devices obtain a high hole mobility of 0.627 cm^2 V^{-1} s^{-1}. The results demonstrate that DTTT-T-DPP based random polymers are promising candidates for various high-performance

organic electronic devices. What is more, the strategy of designing new D/A molecules on the basis of high-performance structures is proved effective.

Keywords: thin film transistors; random polymers; alternative polymers; polymer solar cells

Introduction

The development of new conjugated polymers bring rapidly progress for polymer thin-film transistors (PTFTs) and polymer solar cells (PSCs).[1-4] The significant increase in device performance largely originates from the successful development of new semiconducting materials with extended π-conjugation.[5,6] Of the wide range of semiconducting polymers developed, donor-acceptor (D-A) type polymers which alternate a conjugated electron-rich donor (D) unit with a conjugated electron-deficient acceptor (A) unit in the same polymer backbone have emerged as a promising class of materials.[7-9] Therefore, the creating of excellent building blocks for constructing D-A polymers is particularly crucial to reach high device performance. Among those superior blocks in high performing materials, diketopyrrolopyrrole (DPP) is one of the most versatile and widely used structural motifs.[10-14]

As a polar bicyclic lactam electron-deficient unit, DPP exhibits off-axis dipoles along the polymer backbone, which have been known to promote intermolecular interaction.[4] Meanwhile, as the result of interactions between the sulfur atom on the flanked thiophene and the oxygen atom on lactam ring (S-O), DPP unit has low conformational disorder leading to highly coplanarity in polymer chains.[1] At the same time, for the purpose of constructing excellent D-A polymer based on DPP molecule, the appropriate donor units are also extremely required to be exploited. Specially, a donor possessing the analogous structure with DPP molecule maybe is promising in view of the outstanding properties of DPP.

To date, the donor part copolymerized electron-deficient DPP unit with the thiophene (T) and thieno[3,2-b]thiophene (TT) has afforded high mobility materials for PTFT devices.[13,14] Inspired by this, a novel donor unit 3,6-di(thiophen-2-yl)thieno[3,2-b]thiophene (DTTT) based on T and TT, where the TT core is flanked by thiophene at the 3, 6-position of TT, has been designed and synthesized to imitate the geometry feature of DPP molecule. Similar to DPP molecule, the interactions between the sulfur atoms on T and TT unit (S-S) are

supposed to favor a high degree of planarity and facilitate charge transport. By combination of the fused aromatic DTTT and DPP blocks, the new D-A conjugated copolymer is expected to obtain superior charge transporting ability and photovoltaic performance. However, most of DPP-based alternating polymers failed to achieve high organic photovoltaics (OPV) device performance due to their high highest occupied molecular orbital (HOMO) level over -5.2 eV as well as the low open-circuit voltage (V_{oc}) about 0.6 V. Thus, the frontier orbital energy levels of DPP-based D-A copolymers need to be further adjusted carefully. Comparing with D-A alternating polymerization, D-A randomly copolymerization is more excellent in controlling energy levers of the copolymers by tailoring the co-monomer (donor, acceptor, or linking unit) feed ratio.[15,16] Nevertheless, according to our previous study, the charge-transport properties and device performance of random copolymers are strongly influenced by the molecular geometry of both donor and accept molecules. The difference in molecular geometry between donor and acceptor will be magnified through random polymerization, resulting in the poor performance. In this sense, the structure similarity of the DTTT and DPP can avoid the negative effect caused by the molecular geometry difference. In addition, the involving of simple conjugated molecule (such as thiophene) as linking unit will not affect the primary molecule structures.

Based on above mentioned aspects, choosing the thiophene as the linking unit, random copolymers, poly{3,6-di(thiophen-2-yl)thieno[3,2-b]thiophene-thiophene-3,6-di- (thiophen-2-yl)pyrrolo[3,4-c]pyrrole-1,4(2H,5H)-dione} (PDTTT-T-DPP), were synthesized with two different feed ratios of DTTT/DPP of 3/7 and 4/6, namely PDTTT-T-DPP_3/7 and PDTTT-T-DPP_4/6. As reported in literature and our previous study[15], the little more content of acceptor unit (DPP) than donor unit (DTTT) was beneficial for device performance, thus two feed ratios of 3/7 and 4/6 were selected. Moreover, the corresponding alternating polymer poly{3,6-di(thiophen-2-yl)thieno[3,2-b]thiophene-alt- 3,6-di-(thiophen-2-yl)pyrrolo[3,4-c]pyrrole-1,4(2H,5H)-dione}(PDTTT-DPP) was also

prepared by direct arylation scheme starting from 2,5-dioctyl-3,6-di(thiophen-2-yl)thieno[3,2-b]thiophene (DTTT) and 3,6-bis(5-bromothiophen-2-yl)-2,5-bis(2-octyldodecyl)pyrrolo[3,4-c]pyrrole-1,4(2H,5H)-dione (dibromo-DPP) as monomers.[17] The comparison between the PDTTT-T-DPP with random arrangement and alternating polymer PDTTT-DPP on charge transport properties and photovoltaic performance has been given special attention.

Results and discussion

Synthesis and characterization of the monomer and copolymers

The detailed synthetic routes and chemical structures of the monomers and copolymers are described in **Scheme 1** and the **Supporting Information** (**SI**). A simple 2,5-bis(tributylstannyl)thiophene molecule was employed as the bridge to construct D-A random copolymers with brominated DTTT and DPP through Stille coupling polymerization, using tris(dibenzylideneacetone)dipalladium ($Pd_2(dba)_3$) catalyst and tri-o-tolylphosphine ligand ($P(o\text{-}Tolyl)_3$). In addition, the alternating polymer PDTTT-DPP was prepared by direct arylation using palladium acetate ($Pd(OAc)_2$), potassium carbonate (K_2CO_3) and anhydrous dimethylacetamide (DMAc). To ensure sufficient solubility and self-organization, linear chain octyl and branched 2-octyldodecyl side chains were substituted on DTTT and DPP unit, respectively. These resulted copolymers are highly soluble (~20 mg/ mL) in common organic solvent such as chloroform, chlorobenzene and chloronaphthalene. The structures of monomer and the polymers have been confirmed by ^1H NMR and ^{13}C NMR spectra, as shown in **SI** (**Figure S1-S11**). Molecular weights of the polymers were determined by gel permeation chromatograph (GPC) and the data are listed in **Table S1**. Seen from it, the D-A random copolymers, PDTTT-T-DPP_3/7 and PDTTT-T-DPP_4/6, are apt to gain higher molecular weight. The number average molecular weight (M_n) of them is 17.6 and 14.7 kg/mol respectively, with polydispersity index (PDI) of 2.13 and 2.32, whereas the M_n of D-A alternating copolymer PDTTT-DPP is only 10.8 kg/mol with smaller PDI of 1.65. Moreover, by

comparing the respective integration of the H atom on the side chain (S-C-C-H and N-C-H) of DTTT and DPP, the actual compositions of the random polymers were calculated and the date was also shown in **Table S1**, which were consistent with feed ratios of the co-monomers. The thermal parameters were also presented in **Figure S12, Figure S13** and **Table S1**. All the three polymers displayed similar high decomposition temperature (5% weight loss, T_d), close to 400°C, regardless of the polymerization pattern or the molecular weight.

Optical and electrochemical properties

Figure 1(a) shows the UV-visible absorption spectra of the polymers in dilute chloroform solution and in solid film. The polymers PDTTT-T-DPP_3/7 and PDTTT-T-DPP_4/6 exhibit the similar absorption spectra, while PDTTT-DPP shows much different absorption spectrum. As listed in **Table 1**, the absorption maximum of PDTTT-T-DPP_3/7, PDTTT-T-DPP_4/6 and PDTTT-DPP are located at 710 nm, 752 nm, and 650 nm respectively in solution. From solution state to solid film, the absorption peaks of all these three polymers are red-shifted. Obviously, the random polymers show the red-shifted peaks compared to the alternating counterpart, suggesting that PDTTT-T-DPP_3/7 and PDTTT-T-DPP_4/6 have more efficient conjugation with the backbone due to the insertion of extra thiophene, meaning that higher performance may be obtained in the devices. Detailedly, the three polymers show near absorption edges at long wavelength direction and the optical band gaps (E_g^{opt}) are 1.36 eV for PDTTT-T-DPP_3/7, 1.37 eV for PDTTT-T-DPP_4/6, and 1.32 eV for PDTTT-DPP.

The HOMO and LUMO (Lowest Unoccupied Molecular Orbital) level values of these polymers were estimated from electrochemical cyclic voltammetry (CV) measurement. **Figure S14** shows the CV plots and the related data are presented in **Table 1**. The HOMO/LUMO levels were calculated to -5.21/-3.63 eV for PDTTT-T-DPP_3/7, -5.25/-3.60 eV for PDTTT-T-DPP_4/6, and -5.17/-3.71 eV for PDTTT-DPP from onset oxidation potentials (E_{ox}^{onset})/ reduction potentials (E_{red}^{onset}). In order to make a distinct comparison, the energy level diagrams of polymers and

PCBM ([6,6]-phenyl-C_{61}/C_{71}-butyric acid methyl ester) were described in **Figure 1 (b)**. The random polymers PDTTT-T-DPP_3/7 and PDTTT-T-DPP_4/6 show the lower HOMO levels and higher LUMO levels than PDTTT-DPP. The decreased HOMO energy level is expected to be beneficial for increasing stability of the polymer against oxidation as well as enhancing the hole injection from gold source electrode into p-type thin film. Furthermore, the lower HOMO levels and higher LUMO levels of PDTTT-T-DPP_3/7 and PDTTT-T-DPP_4/6 will offer a relatively higher open circuit voltage (V_{oc}) and more efficient charge transfer from electron donor (polymers) to electron acceptor (PCBM).

Theoretical calculation and Crystallinity

Density functional theory (DFT) computation is performed to give a preliminary insight into the electronic structures of DTTT (D) and DPP (A) by using the DFT B3LYP/6-31G(**) level with the Gaussian 09 package. For more convenient simulation, the alkyl groups are replaced by methyl groups, where the electronic properties and equilibrium geometries will not be influenced significantly. [18,19] And each molecule is optimized under several conformations and is determined at their lowest energy. As shown in **Figure 2**, the dihedral angle between the TT unit and flanked thiophene in the single DTTT are 37.2° and -41.4°, while the values for single DPP are -5.1° and -5.2°. Regrettably, the planarity of DTTT structure is not as good as the DPP molecule, which is beyond our original speculation. The molecular simulation is also executed on these polymers with the different arrangements of DTTT-DPP (D-A), DTTT-T-DPP (D-π-A), DTTT-T-DTTT (D-π-D), and DPP-T-DPP (A-π-A) (**Figure 3**). When linking the DTTT with DPP, minor dihedral angle is present between the unit D and A, meanwhile, the high co-planarity of DPP is maintained during the incorporation of the two segments. Adding thiophene (T) to the arrangement of D-A in further, there are not apparent influence on the geometry of molecular backbone. In other words, the construction of random polymer does not distort the plane of backbone in the system. Additionally, the special cases of D-π-D and A-π-A exhibit the different results. For D-π-D, the dihedral angle between every

two neighboring units emerges in relatively high level. However, the A-π-A gets the decrescendo dihedral angle like the D-A or D-π-A did. The results proved that the DTTT/DPP ratios of 3/7 and 4/6 in the study were benefited to keep the chain's planarity, as A-π-A is the dominant arrangement in polymers PDTTT-T-DPP_3/7 and PDTTT-T-DPP_4/6.

X-ray diffraction (XRD) measurements were used to reveal the molecular arrangement of the three polymers in pristine thin films. As shown in the **Figure 4**, the random polymers PDTTT-T-DPP_3/7 and PDTTT-T-DPP_4/6 showed a diffraction peak at 2θ of around 4.5° characteristic of lamellar d-spacing (100 peak) which translates to an inter-lamellar distance of approximately 19.6 Å. While the slightly lower angle of 4° with the larger d-spacing of 21.9 Å was found for PDTTT-DPP with respect to PDTTT-T-DPP_3/7 and PDTTT-T-DPP_4/6. More importantly, the intense and sharp peak (100) for PDTTT-T-DPP_3/7 and PDTTT-T-DPP_4/6 implied the more ordered interlayer packing structure than the PDTTT-DPP. There is also a smaller crystalline peak at 2θ= ~9° in PDTTT-T-DPP_3/7 and PDTTT-T-DPP_4/6, related to the (200) peak. This peak is indicative of increased crystallinity for PDTTT-T-DPP_3/7 and PDTTT-T-DPP_4/6, which is in agreement with the greater intensity of their (100) peaks. It is noticed that a π-π stacking (010) peak at 2θ of around 23° (3.85 Å) existed in PDTTT-DPP, which is favorable for vertical charge transport. However, no clear (010) peak can be observed in the diffraction patterns of PDTTT-T-DPP_3/7 and PDTTT-T-DPP_4/6 films.

Space charge limited current (SCLC) measurement

Hole-only devices were specifically fabricated to estimate the charge mobility of pure polymers and polymers/PCBM blend films by SCLC model with a device configuration of glass/ITO/PEDOT:PSS/polymers(or polymer:PCBM)/MoO_3/Ag. The fabrication procedure is described in the experimental section and **Figure S15** exhibits the hole-only dark I-V curves. In pristine films, the calculated hole mobility values of PDTTT-T-DPP_3/7, PDTTT-T-DPP_4/6, and PDTTT-DPP are 2.3×10^{-2} cm^2 V^{-1} s^{-1},

1.1×10^{-2} cm^2 V^{-1} s^{-1}, and 7.0×10^{-3} cm^2 V^{-1} s^{-1}, respectively. The PDTTT-DPP exhibits the lowest mobility is surprising since the XRD measurement shows the better π-π stacking between polymer PDTTT-DPP chains. On the other hand, although there are not evident difference on optical, electrochemical and crystalline properties between PDTTT-T-DPP_3/7 and PDTTT-T-DPP_4/6, PDTTT-T-DPP_3/7 achieves higher mobility compared to PDTTT-T-DPP_4/6, which probably results from the PDTTT-T-DPP_3/7 containing more content of the preferable planarity DPP unit. As listed in **Table S2**, after blending with PCBM, the hole mobility of these polymers are down-shifted. The blend film of PDTTT-T-DPP_3/7:PCBM gets the highest mobility as expected. Since the collected current is dependent on the charge transporting properties of the bulk heterojunction (BHJ) layer, the higher hole mobility may be translate to the larger J_{sc} for the PDTTT-T-DPP_3/7 based device. Moreover, PDTTT-DPP and PCBM blend film reveals the lowest mobility, suggesting that morphology of PDTTT-DPP film and PDTTT-DPP/PCBM blend film is unsatisfactory. Furthermore, the mobility of polymer and $PC_{71}BM$ blend obtained the similar values of polymers and $PC_{61}BM$ blend, despite the better charge transport property of $PC_{71}BM$ relative to $PC_{61}BM$.

Polymer thin film transistors (PTFTs) measurement

Bottom-gate top-contact (BGTC) PTFTs were fabricated to investigate the charge transport properties of random and alternating polymers, represented by PDTTT-T-DPP_3/7 and PDTTT-DPP respectively. The channel width (W) was 1400 μm and different channel lengths (L) of TFT devices (from 5 to 50μm) were investigated to optimize device performance. **Table 2** lists the extracted electrical parameters of PTFTs device. **Figure 5** presents the typical output and transfer curves of PDTTT-T-DPP_3/7-based TFT devices, and the corresponding curves for PDTTT-DPP were shown in **Figure S16**. All devices with L=50 μm (W/L=28) exhibits the optimal hole mobility, as shown in the **Table S3**. At the room temperature, PDTTT-T-DPP_3/7 shows high hole mobility of 0.460 cm^2 V^{-1} s^{-1}, with a threshold voltage (V_{th}) of -3.2 V and an notable on/off ratio ((I_{on}/I_{off}) of 4.6×10^6. In contrast, a

hole mobility of 7.55×10^{-3} cm^2 V^{-1} s^{-1} ($I_{on}/I_{off}=2.3\times10^5$, V_{th}=-19.4 V) was obtained for a PDTTT-DPP-based PTFT device. The higher hole mobility of PDTTT-T-DPP_3/7 should be related to the better backbone co-planarity and strong layer interaction observed from UV, theoretical calculations and XRD measurement. Moreover, the molecular weight played a key role in improving charge mobilities, because the thin film crystallinity could be enhanced with growing molecular weight.[20] The relatively low molecular weight for PDTTT-DPP compared with PDTTT-T-DPP_3/7 also should pay for the lower hole mobility. Furthermore, on account of that the thermal annealing was beneficial to improve the charge mobility as reported in many literatures [21-23], the field-effect hole mobility was also investigated after thermal annealing at various temperatures for 1 h in vacuum. With a rise in annealing temperature from 100 to 200 °C, the hole mobility of PDTTT-T-DPP_3/7-based device tended to increase, and afforded the highest hole mobility of 0.627 cm^2 V^{-1} s^{-1} after annealing at 200 °C, with an on/off ratio of 2.9×10^6. In general, when TFT devices are annealed, the residual oxygen and moisture (H_2O) trapped at the interfaces are released. This will lead to a shift in the V_{th} to a smaller value and then facilitating the hole transport. [24] Similarly, device using PDTTT-DPP shows the same variation. After annealing, PDTTT-DPP-based devices give the high hole mobility of 2.11×10^{-2} cm^2 V^{-1} s^{-1} at 100 °C and 3.51×10^{-2} cm^2 V^{-1} s^{-1} at 200 °C.

Photovoltaic Characteristics

Single-junction solar cells were fabricated using the inverted device structure ITO/ZnO/polymers:PCBM ($PC_{61}BM$ or $PC_{71}BM$)/MoO_3/Ag. Solutions prepared used different solvents such as chlorobenzene (CB), 1-chloronaphthalene (CN), and their mixed solvent. The parameters of devices with best efficiency are listed in **Table 3** and all results are summarized in **Table S4.** For the polymer solar cells (PSCs) devices processed from pristine CB solution (**Figure S17**), the PDTTT-T-DPP_3/7-based devices exhibit the inferior PCE compared to PDTTT-T-DPP_4/6, due to the lower short-circuit current (J_{sc}) and fill factor (FF). Because there are delicate differences in photoelectric properties between

PDTTT-T-DPP_3/7 and PDTTT-T-DPP_4/6, we speculated that the origin behind poor performance of PDTTT-T-DPP_3/7 should be correlated to the unfavorable blend film morphology spin-coating from CB solution. As the acceptor varied from $PC_{71}BM$ to $PC_{61}BM$, the enhancement of J_{sc} which multiplied from ~3 mA·cm^{-2} to ~6 mA·cm^{-2}, may stem from the lower LUMO level of $PC_{61}BM$ than that of $PC_{71}BM$, as larger energy difference between the LUMO levels of the donor polymer and $PC_{61}BM$ will facilitate efficient exciton splitting and charge dissociation. In addition, the poor PCE appeared in the PDTTT-DPP-based devices is probably due to the worse and discontinuous active layer film even in macroscopical view, originating from its poor film-forming property with PCBM.

Generally, CN as the additive will improve the morphology of mixtures of low band gap polymers with PCBM, and in recently report, CN even can be used as the single solvent to enhance the device performance.[25] Thus, the PSCs processed from pristine CN solution were prepared. Use the CN as solvent, solar cells made from PDTTT-T-DPP_3/7:$PC_{61}BM$ achieve an obviously increased PCE of 2.7% with a J_{sc} of 7.638 mA·cm^{-2}, V_{oc} of 0.587 V, and FF of 59.6%, which is 80% enhancement over the CB solvent device (**Figure 6**). However, the CN solvent device based on PDTTT-T-DPP_4/6 only obtains a slightly improved PCE. Thus it can be seen that, when the film morphology get optimized, the advantageous hole mobility of PDTTT-T-DPP_3/7 helps its device to achieve the better PCE. In order to further increase the PCE from the positive function of CN solvent, devices with the active layer prepared from CB with different concentrations of CN as additive were fabricated, the related data were present in **Table S4**. Although the PCEs from the PSCs based on these polymers processed from CB solutions with increasing concentrations of CN are higher than that from pristine CB solution, a higher PCE than 2.7 % did not obtained. On the other side, although the energy levels have been tuned via random copolymerization in this work, the relative high HOMO levels (~5.20 eV) and low LUMO levels (~3.65 eV) of these polymers are still not appropriate enough, which should be a reason for the imperfect PCE in PSCs device.

Morphology study

The surface morphology properties of the polymer:PCBM blend films were tested by using atomic force microscopy (AFM) to understanding the significant effect of CB and CN solvents, and the size of AFM is 5×5 μm^2. **Figure 7** and **Figure S18** show the typical height images and phase images of polymers (PDTTT-T-DPP_3/7 and PDTTT-T-DPP_4/6):PCBM ($PC_{61}BM$ and $PC_{71}BM$) blend films respectively, and the 3D images are presented in **Figure S19**. Notably, all the PDTTT-T-DPP_3/7-based films processed from CB solvent exhibited large grains and the less grain-boundary density with the root-mean-square (RMS) roughness excess 7 nm, which implied the reduced the heterojunction interface area for exciton dissociation and consequently led to the low J_{sc} of the their OPVs. For PDTTT-T-DPP_4/6, their films also show certain aggregation, but for their smaller RMS values (about 5 nm) and more continuous phase-separation observed from 3D images compared with PDTTT-T-DPP_3/7 film, the OPVs based on PDTTT-T-DPP_4/6 from CB solvent obtains the better performance. When prepared from CN solvent, the blend films formed fine granular domains with a RMS roughness of about 3 nm. Obviously, the large heterojunction interfaces and sufficient percolation paths can be realized to facilitate the charge transport as well as the devices efficiency. Moreover, the film of PDTTT-T-DPP_3/7:$PC_{61}BM$ consisted of intertwined grains, which is of great benefit to decrease photocurrent recombination and accelerate charge transport. Consequently PDTTT-T-DPP_3/7:$PC_{61}BM$ achieved the best PCE with the highest J_{sc}.

Conclusion

In conclusion, we designed and synthesized a novel D-A donor di(thiophen-2-yl)thieno[3,2-b]thiophene (DTTT) according to the structure of diketopyrrolopyrrole (DPP). Use the DPP as the acceptor and thiophene as the linking unit, the random polymers PDTTT-T-DPP_3/7, PDTTT-T-DPP_4/6 and the alternating polymer PDTTT-DPP were synthesized through the random copolymerization and direct arylation scheme respectively. Although the planarity of DTTT structure is not as good as the DPP molecule, incorporating of DTTT and DPP

molecule prompts the polymers to achieve the high hole mobility, especially for PDTTT-T-DPP_3/7. Polymer thin film transistors (PTFTs) devices based on PDTTT-T-DPP_3/7 obtains a high hole mobility of 0.627 cm^2 V^{-1} s^{-1} and the corresponding space charge limited current (SCLC) measurement also show the high hole mobility of 2.3×10^{-2} cm^2 V^{-1} s^{-1}. Besides, PDTTT-T-DPP_3/7:$PC_{61}BM$ obtains a PCE of 2.7%. Thus, the design of the new donor unit DTTT and its random copolymers with DPP molecule is reasonable, demonstrating that the negative effect of molecular geometry on the random copolymer can be weakened by selecting the suitable structure of donor and acceptor. Therefore, via the random copolymerization, more D/A blocks can be designed and synthesized, by imitating those excellent structures, to further boost the performance of organic electronic devices efficiently.

Electronic Supplementary Information (ESI) available

Text giving ^1H NMR and ^{13}C NMR spectra of the monomers and polymers, thermal properties and molecular weights of the random and alternative polymers, CV plots and X-ray diffraction of the polymers, the hole-only dark I-V curves of the random and alternative polymers, typical output and transfer curves for PDTTT-DPP of PTFTs device, I-V curves of PSCs devices processed from pristine CB solution, typical phase images and 3D images of polymers (PDTTT-T-DPP_3/7 and PDTTT-T-DPP_4/6):PCBM ($PC_{61}BM$ and $PC_{71}BM$) blend films. This information is available free of charge via the Internet at http://pubs.rsc.org.

Acknowledgements

This work was financially supported by the National Science Fund for Distinguished Young Scholars (51425304), National Natural Science Foundation of China (51273088, 51263016 and 51473075), and National Basic Research Program of China (973 Program 2014CB260409).

Reference

[1] Nielsen, C. B.; Turbiez, M.; McCulloch, I. *Adv. Mater*. **2013**, 25, 1859.

[2] Guo, X.; Zhou, N.; Lou, S.; Smith, J.; Tice, D. B.; Hennek, J. W.; Ortiz, R. P.; Navarrete, J. T. L.; Li, S.; Strzalka, J.; Chen, L.; Chang, R. P. H.; Facchetti, A.; Marks, T. J. *Nat. Photonics* **2013**, 7, 825.

[3] Small, C. E.; Chen, S.; Subbiah, J.; Amb, C. M.; Tsang, S.-W.; Lai, T.-H.; Reynolds, J. R.; So, F. *Nat. Photonics* **2012**, 6, 115.

[4] Bijleveld, J. C.; Zoombelt, A. P.; Mathijssen, S. G. J.; Wienk, M. M.; Turbiez, M.; de Leeuw, D. M.; Janssen, R. A. J. *J. Am. Chem. Soc.* **2009**, 131, 16616.

[5] Chen, H.; Guo, Y.; Yu, G.; Zhao, Y.; Zhang, J.; Gao, D.; Liu, H.; Liu, Y. *Adv.Mater.* **2012**, 24, 4618.

[6] Li, J.; Zhao, Y; Tan, H.; Guo, Y.; Di, C.-A.; Yu, G.; Liu, Y.; Lin, M.; Lim, S. H.; Zhou, Y.; Su, H.; Ong. B. S. *Sci. Rep.* **2012**, 2,754.

[7] Liu, Y.; Zhao, J.; Li, Z.; Mu, C.; Ma, W.; Hu, H.; Jiang, K.; Lin, H.; Ade, H.; Yan, H. *Nat. Commun* **2015**, 5, 5293.

[8] Wang, N.; Chen, Z.; Wei,W.; Jiang, Z. *J. Am. Chem. Soc.* **2013**, 135, 17060.

[9] Nguyen, T. L.; Choi, H.; Ko, S.-J.; Uddin, M. A.; Walker, B.; Yum, S.; Jeong, J.-E.; Yun, M. H.; Shin, T. J.; Hwang, C. S.; Kim, J. Y.; Woo, H. Y. *Energy Environ. Sci.* **2014**, 7, 3040.

[10] Hugo, B.; Elisa, C-F.; Afshin H.; Ying, W. S.; Huang, Z.; Stoichko, D. D.; Raja, S. A.; Barry, P. R.; Scott, E. W.; Pabitra, S. T.; Iain, M.; James, R. D.; Iain M. *Adv. Funct. Mater.* **2013**, 23, 5647.

[11] Li, W.; Hendriks, K. H.; Christian Roelofs, W. S.; Kim, Y.J.; Wienk, M. M.; Janssen, R. A. J. *Adv. Mater.* **201**3, 25, 3182.

[12] Cho, M. J.; Shin, J.; Yoon, S. H.; Lee, T. W.; Kaur, M.; and Choi, D. H. *Chem. Commun*. **2013**, 49, 7132.

[13] Meager, I.; Ashraf, R. S.; Rossbauer, S.; Bronstein, H.; Donaghey, J. E.; n Marshall, J.; Schroeder, B. C.; Heeney, M.; Anthopoulos, T. D.; McCulloch, I. *Macromolecules*. **2013**, 46, 5961.

[14] Wang, Y.; Yang, F.; Liu, Y.; Peng, R.; Chen, S.; Ge. Z. *Macromolecules* **2013**, 46, 1368.

[15] Deng, Z.; Chen, L.; Wu, F.; Chen. Y. *J. Phys. Chem. C.* **2014**, 118, 6038.

[16] Kang, T. E.; Cho, H-H.; Kim, H. J.; Lee, W.; Kang, H.; Kim. B. J. *Macromolecules*. **2013**, 46, 6806.

[17] Sebastian, K.; Sybille, A.; Ullrich, S. *ACS Macro Lett.* **2012**, 1, 465.

[18] Frisch, M. J.; Trucks, G. W.; Schlegel, H. B.; Scalmani, G.; Barone, V.; Ortiz, J. V.; Cioslowski, J.; Fox, D. J. Gaussian 09; Revision A.01; Gaussian, Inc.: Wallingford, CT, **2009**.

[19] Peng, Q.; Lim, S. L.; Wong, I. H.; Xu, J.; Chen, Z. K.. *Chem. - Eur. J.* **2012**, 18, 12140.

[20] Tsao, H. N.; Cho, D. M.; Park, I.; Hansen, M. R.; Mavrinskiy, A.; Yoon, D. Y.; Graf, R.; Pisula, W.; Spiess, H. W.; Mu¨ llen, K. *J. Am. Chem. Soc.* **2011**, 133, 2605.

[21] Kim, G.; Kang, S-J.; Dutta, G. K.; Han, Y-K.; Shin, T. J.; Noh, Y-Y.; Yang, C. *J. Am. Chem. Soc.* **2014**, 136, 9477.

[22] Yum, S.; An, T. K.; Wang, X.; Lee, W. Uddin, M. A.; Kim, Y. J.; Nguyen, T. L.; Xu, S.; Hwang, S.; Park, C.; Woo; H. Y. *Chem. Mater.* **2014**, 26, 2147.

[23] Liu, Y.; Liu, F.; Klivansky, L. M.; McGough, A. M.; Zhang, B. A.; Lo, K.; Russell, T. P.; Wang, L.; Liu. Y.; *J. Am. Chem. Soc.* **2014**, 136, 15093.

[24] Wang, Y.; Kadoya, T.; Wang, L.; Hayakawa, T.; Tokita, M.; Mori, T.; Michinobu, T. *J. Mater. Chem. C*, **2015**, 3, 1196.

[25] Yi, C.; Hu, X.; Liu, H. C.; Hu, R.; Hsu, C-H.; Zheng, J.; Gong, Xiong *J. Mater. Chem. C*, **2015**, 3, 26

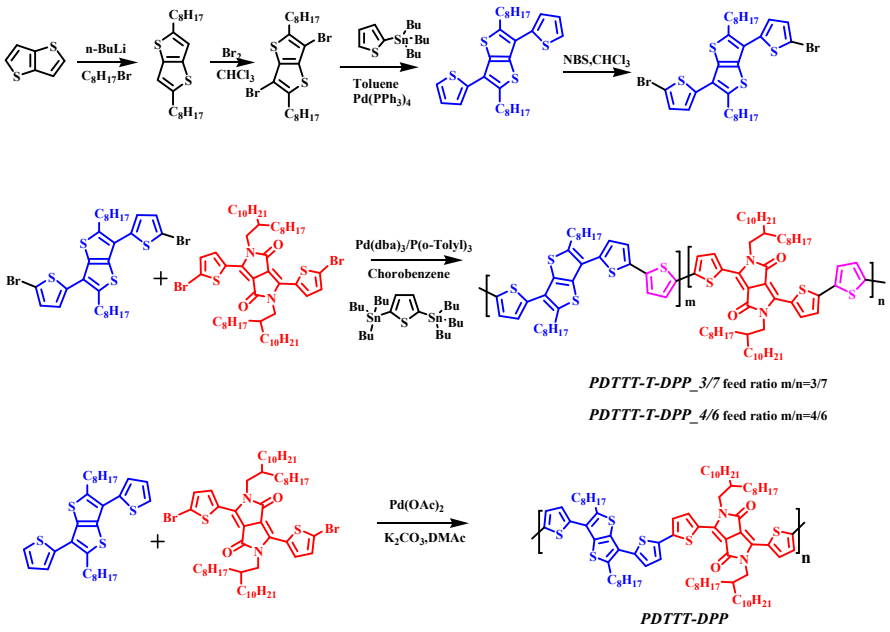

Scheme 1. The structure and synthesis route of monomers and polymers

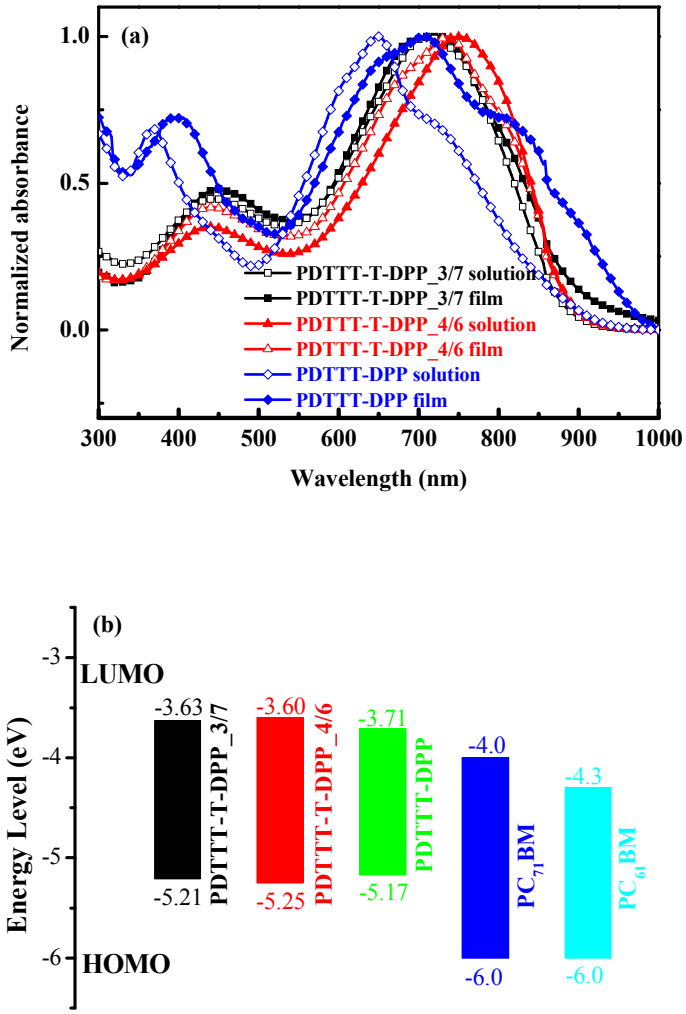

Figure 1. (a) Absorption spectra of three polymers in dilute chloroform solution (open) and in solid film (solid); (b) The energy level diagrams of polymers and PCBM

Table 1. Optical and electrochemical properties of these three polymers

Polymer	Solution λ_{max} (nm)	Film λ_{max} (nm)	λ_{onset}	E_g^{opt} (eV)	E_{ox}^{onset}	HOMO	E_{red}^{onset}	LUMO	E_g^{el}(eV)
PDTTT-T-DPP_3/7	440,710	448,726	912	1.36	0.81	-5.21	-0.77	-3.63	1.58
PDTTT-T-DPP_4/6	445,736	440,752	902	1.37	0.85	-5.25	-0.80	-3.60	1.65
PDTTT-DPP	370,650	400,706	940	1.32	0.77	-5.17	-0.69	-3.71	1.46

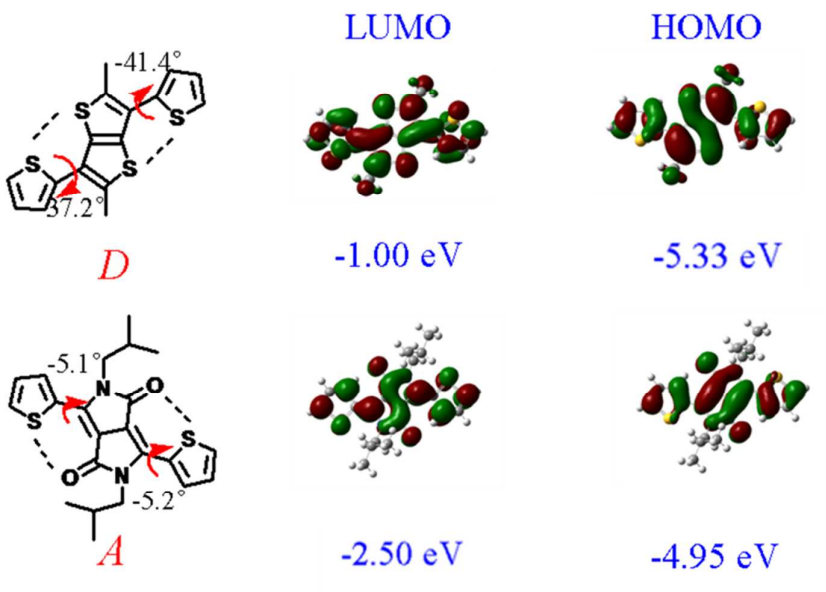

Figure 2. The structure comparison of DPP and DTTT

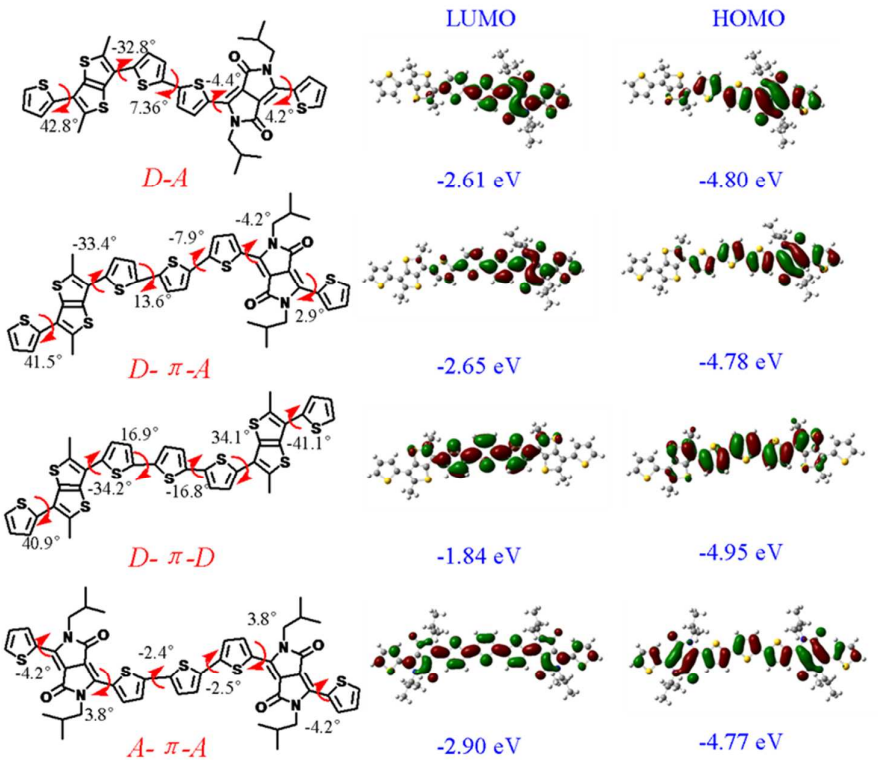

Figure 3. The calculated results of D-A, D-π-A, D-π-D, and A-π-A models

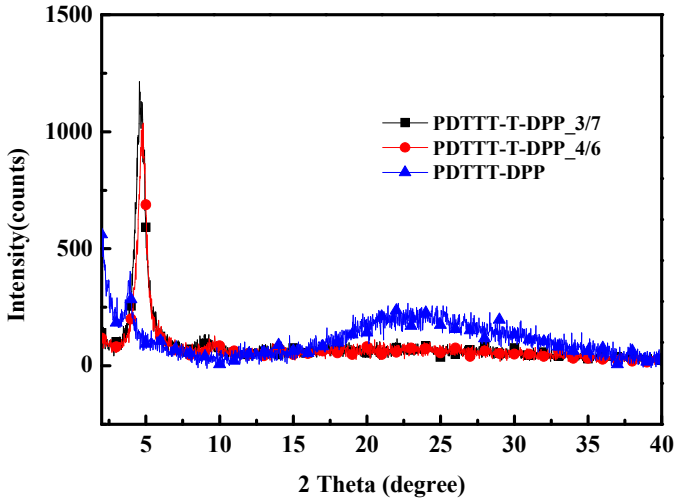

Figure 4. X-ray diffraction patterns of the pristine polymer films (films drop casted onto Si substrates)

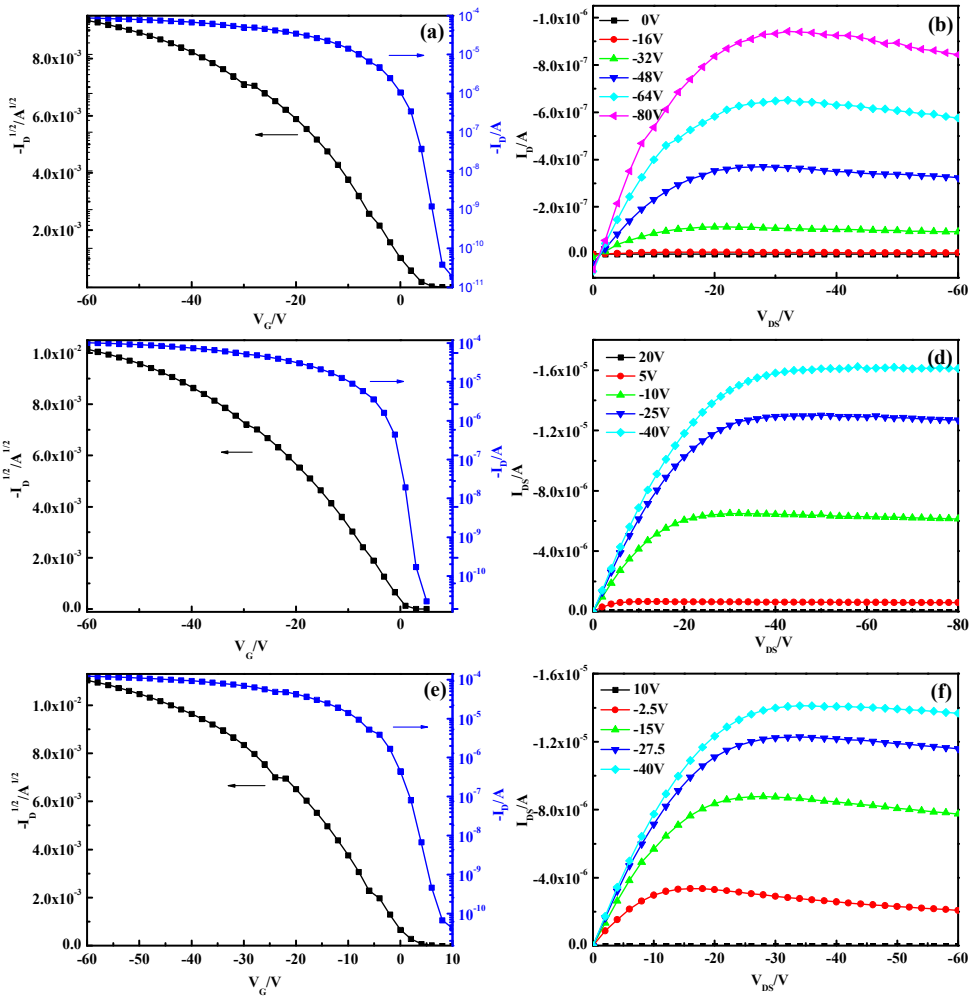

Figure 5. The transfer (a, c, e) and output (b, d, f) characteristics of PDTTT-T-DPP_3/7 films deposited on substrate (a, b), annealed at 100 °C (c, d) and 200 °C (e, f)

Table 2. PTFT Characteristics of copolymers of PDTTT-T-DPP_3/7 and PDTTT-DPP

Polymer	T(°C)	μ ($cm^2 V^{-1} s^{-1}$)	I_{on}/I_{off}	V_{th} (V)
PDTTT-T-DPP_3/7	RT[a]	0.460	4.6×10^6	-3.2
	100	0.572	4.6×10^6	-7.8
	200	0.627	2.9×10^6	-10.4
PDTTT-DPP	RT	7.55×10^{-3}	2.3×10^5	-19.4
	100	2.11×10^{-2}	9.4×10^5	-15.6
	200	3.51×10^{-2}	2.2×10^6	-20.3

[a]Room temperature

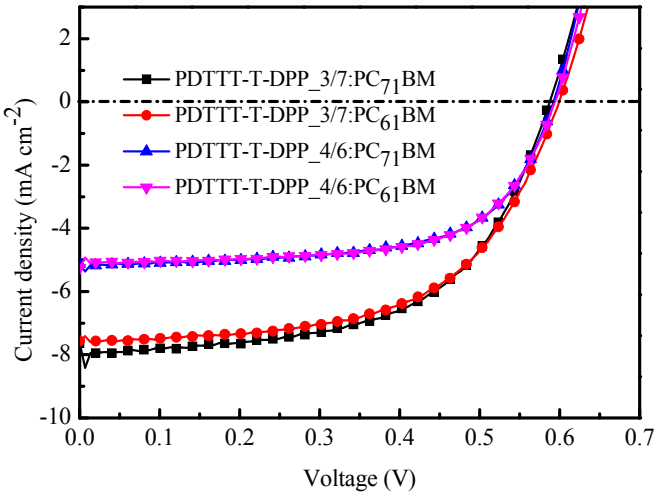

Figure 6. Characteristic J-V curves of the BHJ solar cell based on PDTTT-T-DPP_3/7 and PDTTT-T-DPP_4/6 fabricated from CN

Table 3. Photovoltaic performance of polymers in invert BHJ devices

Polymer	Solvent	Acceptor	Polymer/ PCBM(w/w)	J_{sc} ($mA \cdot cm^{-2}$)	V_{oc} (V)	FF (%)	PCE (%)
PDTTT-T-DPP_ 3/7	CN	$PC_{71}BM$	1:1.5	7.565 ±1.582	0.598 ±0.001	57.9 ±0.2	2.6 ±0.4
PDTTT-T-DPP_ 3/7	CN	$PC_{61}BM$	1:2	7.638 ±1.245	0.587 ±0.001	59.6 ±0.2	2.7 ±0.2
PDTTT-T-DPP_ 4/6	CN	$PC_{71}BM$	1:1.5	5.132 ±1.365	0.592 ±0.001	63.8 ±0.3	1.9 ±0.4
PDTTT-T-DPP_ 4/6	CN	$PC_{61}BM$	1:2	5.252 ±1.387	0.594 ±0.001	62.6 ±0.2	2.0 ±0.4
PDTTT-DPP	CB	$PC_{71}BM$	1:1.5	2.150 ±1.255	0.601 ±0.001	26.7 ±0.6	0.3 ±0.2
PDTTT-DPP	CB	$PC_{61}BM$	1:2	2.570 ±1.212	0.565 ±0.001	31.3 ±0.5	0.5 ±0.1

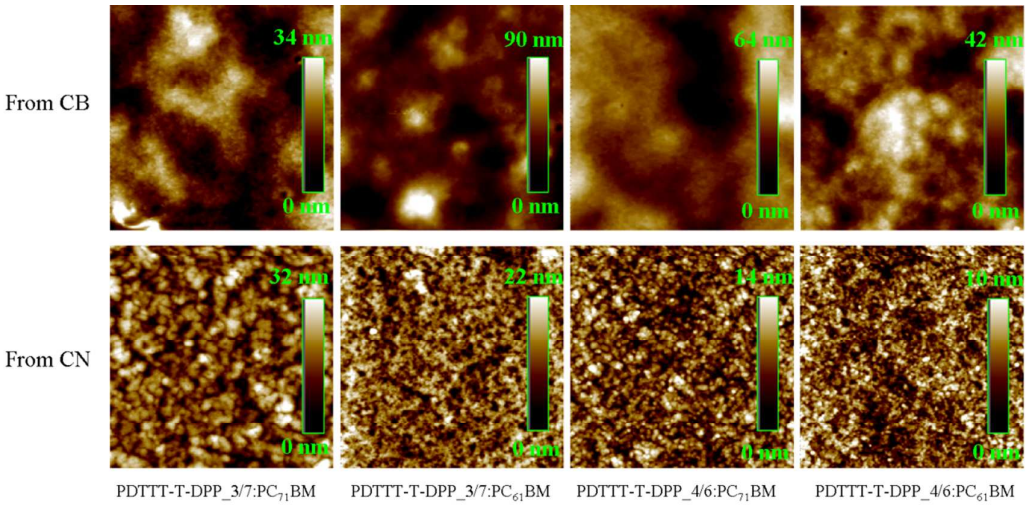

Figure 7. Topography images by AFM of blend films of Polymers:PCBM from different solvents.

Table of content

High Charge Mobility Polymers Based on a New Di(thiophen-2-yl)thieno[3,2-b]thiophene for Transistors and Solar Cells

Lie Chen, Feiyan Wu, Zhiqiang Deng, Linlin Feng, Pengcheng Gu, Huanli Dong, Wenping Hu, Yiwang Chen*

A novel random copolymer of di(thiophen-2-yl)thieno[3,2-b]thiophene (DTTT) with DPP achieved high hole mobility of 0.627 $cm^2 \cdot V^{-1} \cdot s^{-1}$.